Electronic Supplementary Material (ESI) for Nanoscale.

Supplementary Information

Inkjet-printed h-BN memristors for hardware security

Kaichen Zhu,[1-3] Giovanni Vescio,[2] Sergio González-Torres,[2] Julià López-Vidrier,[2] Juan L. Frieiro,[2] Sebastian Pazos[1], Xu Jing,[3] Xu Gao,[3] Sui-Dong Wang,[3] Joaquín Ascorbe-Muruzábal,[4] Juan A. Ruiz-Fuentes,[4] Albert Cirera,[2] Blas Garrido,[2] Mario Lanza[1*]

[1] Materials Science and Engineering Program, Physical Science and Engineering Division, King Abdullah University of Science and Technology (KAUST), Thuwal 23955-6900, Saudi Arabia

[2] MIND, Department of Electronic and Biomedical Engineering, Universitat de Barcelona, Martí i Franquès 1, E-08028 Barcelona, Spain

[3] Institute of Functional Nano & Soft Materials (FUNSOM), Collaborative Innovation Center of Suzhou Nano Science & Technology, Soochow University, 199 Ren-Ai Road, Suzhou 215123, P. R. China

4 Nadetech, Polígono Arbide, Calle V Nave 4, 31110 Noáin, Spain

*Corresponding author email: mario.lanza@kaust.edu.sa

List of Figures

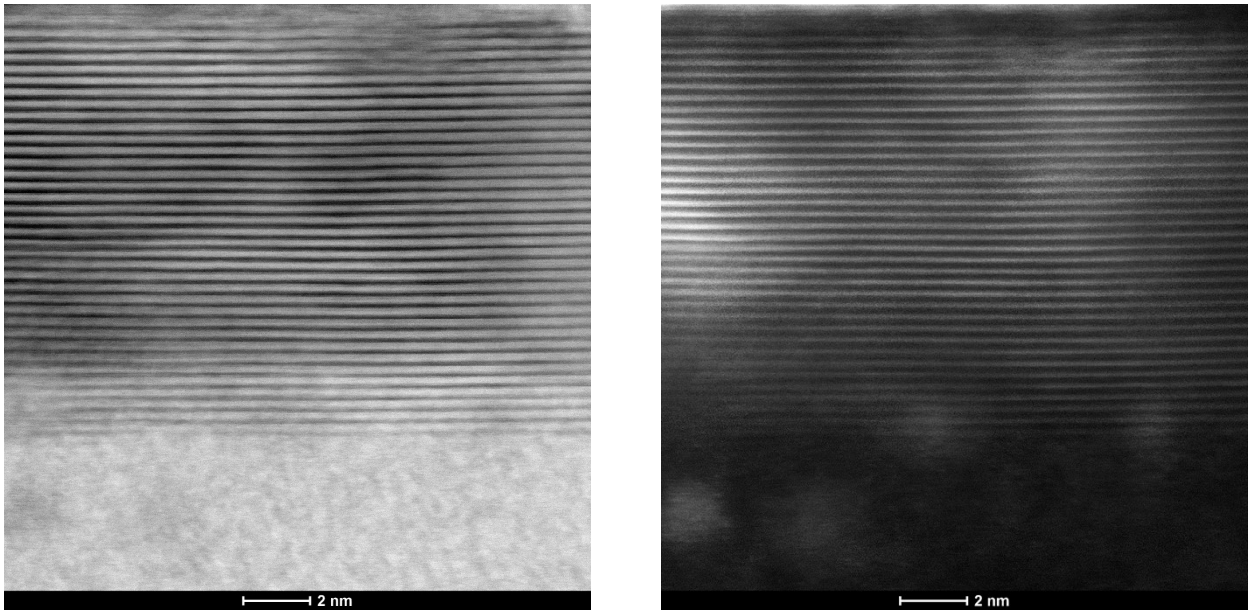

Supplementary Figure 1. The cross-sectional scanning TEM (STEM) images of the same h-BN nanoflake in bright field (BF) mode and high-angle annular dark field (HAADF) mode. In BF image (left), the black lines represent h-BN. In HAADF mode, the white lines represent h-BN.

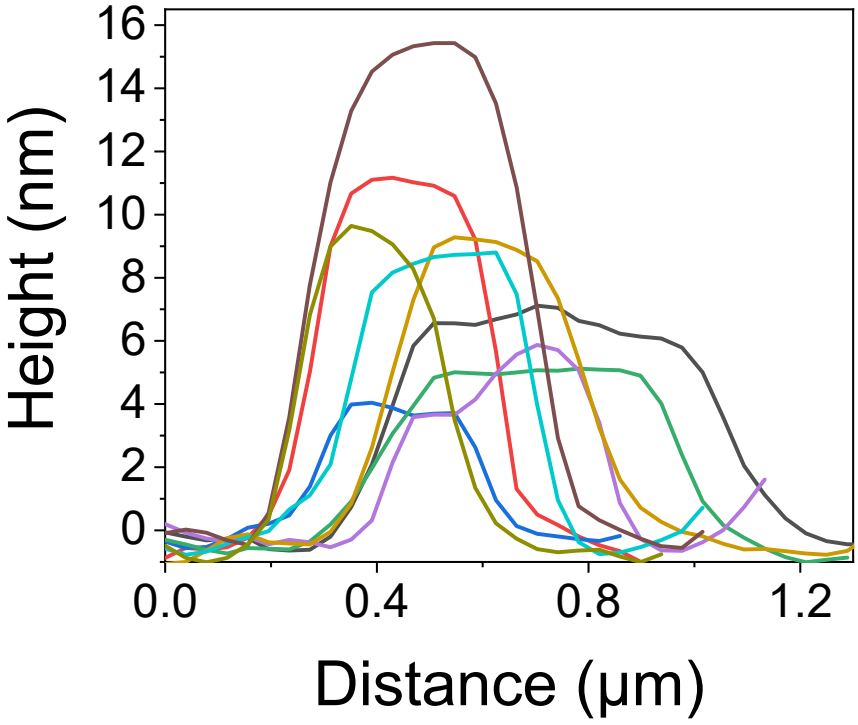

Supplementary Figure 2. Statistical analysis of the thickness and size of the h-BN nanoflakes by AFM profiles from Figure 1c.

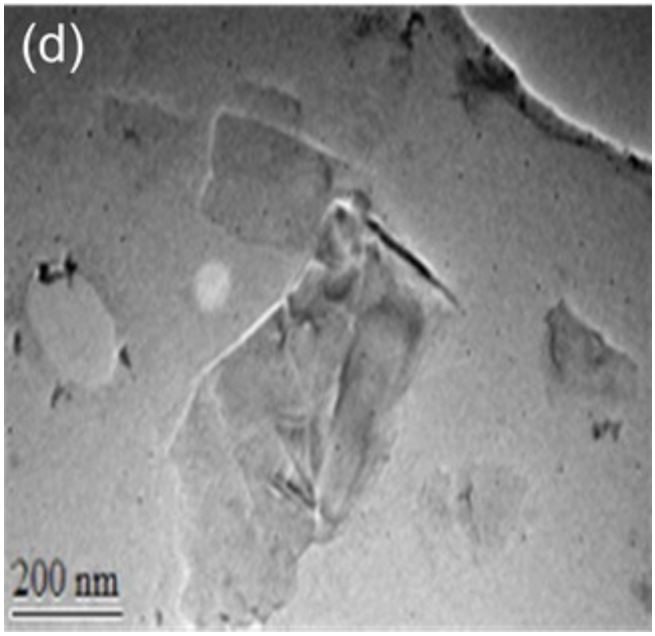

Supplementary Figure 3. Top view TEM image of h-BN nanoflakes.

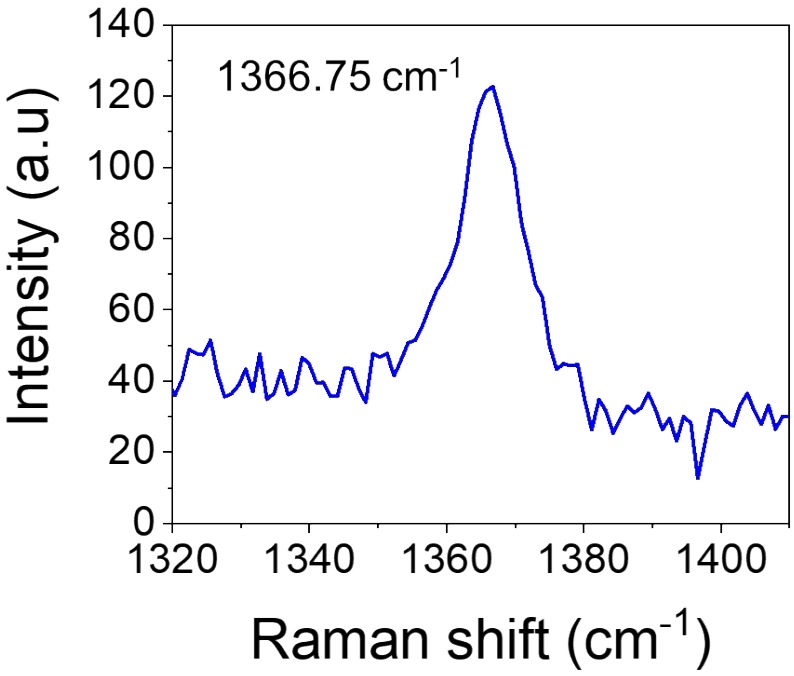

Supplementary Figure 4. Raman spectra of the inkjet-printed h-BN thin film.

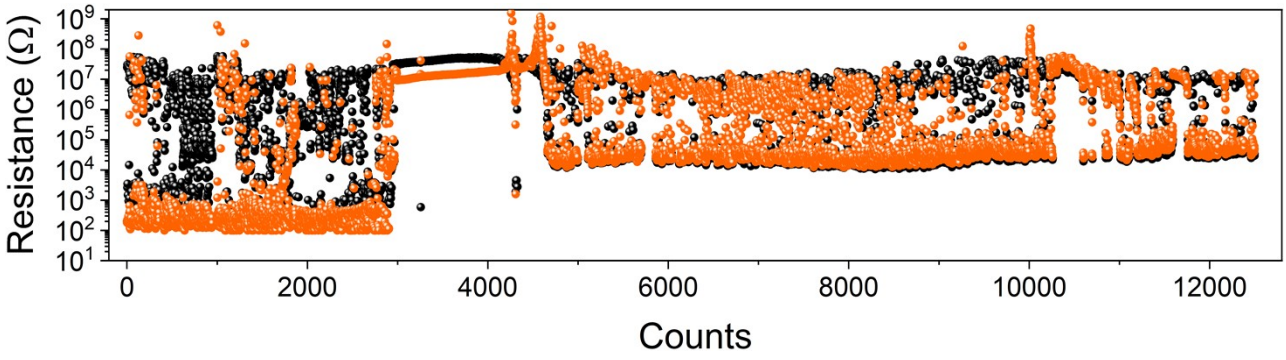

Supplementary Figure 5. Endurance test of Ag/h-BN/Ag memristor showing self-recovery.

Supplementary Table 1: LPE BP based memristor

Ref	**TE/RS medium/BE**	**Print method**	**Endurance**	**data points presented**
1	Al/BP/ITO	Drop-casting	-	-
2	Al/PMMA/BPQDs/PMMA/Al	Sonication exfoliation	100	21
3	Al/BP:PS/Al	Centrifuge	-	-

Supplementary Table 2: LPE GO based memristor

Ref	**TE/RS medium/BE**	**Print method**	**Endurance**	**data points presented**
4	Cu/GO/Pt	Vacuum filtration	100	100
5	Al/GO-PVK/ITO	Toluene-cast	10	9
6	Al/G-O film/Al	Spin-casting	100	21
7	Al/GO/ITO	Spin coating	100	50
8	Al/TPAPAM-GO/ITO	Spin or blade coating	5	-
9	Al/GO/ITO	Spin coating	100	50
10	Al/RGO/ITO	Drop casting	hundreds	8
11	Cu/GO/Pt	Vacuum filtration	-	-
12	Pt/rGO–th/Pt	Vacuum filtration	350	350
13	Al/FPA-rGO/ITO	Spin coating	1000	-
14	Ag/GO/Ag	Spin coating	-	-
15	Al/GO/ITO	Spin coating	100	100
16	Al/GO/p-Si	Spin coating	100	50
	Al/GO/p-Ge		100	50
17	Pt/GO/ITO	Spin coating	100	21
18	Al/rGO/Al	Spin coating	~100	50
19	Ag/HfOx/LSG	Laser-scribing	100	-
20	Ag/GO/ITO	Spin coating	-	-
21	Al/CuO/GO/CuO/Al	Spray-coating	-	-
22	Au/GO/ITO	Spin coating	100	9
23	ITO/RGO/ITO	Dip coating	10^5	-
24	Al/GO/Al	Spin coating	-	-
25	Al/Au NPs-RGO-PVA/ITO	Spin casting	50	-
26	Ag/GO/ITO	Inkjet printing	-	-
27	ITO/GO/ITO/PES	Spin coating	-	-
28	Al/Au NP inserted GO/ITO	Spin coating	10^4	-
29	Ag/GO/rGO/SiO_2/p-Si	Spin coating	100	-
30	Au/GO/Au	Drip	-	-
31	Au/GO/Al	Spin coating	200	-
32	Ag/GO/rGO/Ag	Spin coating	100	-
33	Ag/ZnO-rGO/FTO	Dip coating	-	-
34	Metal/GO/Metal	Spin coating	250	15
35	Pt/Ti/GO/Pt/Ti	Spin coating	10^4	-
36	PEDOT:PSS/GO/PEDOT:PSS	Spin coating	10^3	-
37	Pt/GO/ZnONR/ZnO/ITO	Drop-casting	10^3	-
38	Au/GO/Au	Dripping	-	-
39	Pt/brGO/Pt	Spin coating	-	-
40	Yarns/RGO/Yarns	Spin coating	100	-
41	Ag/N-GO QDs/Pt	Drop-casting	50	-
42	Ag/RGO/ITO	Drop-casting	-	-
43	Al/HGO/ITO	Spin coating	100	-
44	Al/GO-TiO_2/ITO	Spin coating	60	-

45	Pt/ZnO-G/Pt	Spin coating	-	-
46	Ni/PMMA:GO/ITO	Spin coating	300	-
47	Paint/GO/PET	Spin coating	100	15
48	Al/GOAu/ITO	Spin coating	100	-
49	LSMO-rGO	-	10^3	-
50	Al/rGO-ZnO HC/PMMA/ITO	Spin coating	10^3	-
51	Al/GO/Al/PES	Spin coating	100	-
52	Al/GO/Au/GO/ITO	Spin coating	-	20

Supplementary Table 3: LPE MoS_2 based memristor

Ref	**TE/RS medium/BE**	**Print method**	**Endurance**	**data points presented**
55	Al/MoS_2-PVP/(rGO)	Spin coating	-	-
56	rGO/MoS_2/ITO	Spin coating	-	-
57	Ag/MoO_x/MoS_2/Ag	Inkjet, screen printing	10^4	14
58	Al/MoS_2-MoO_x/Al	Spin coating	100	11
59	Au/PMMA/MoS_2 QDs/PMMA/FTO	Spin coating	650	-
60	Al/MoS_2–UCNPs/ITO	Spin coating	200	40
61	Ag/Gr-MoS_2/Cu	Hydrothermal process	500	-
62	Ag/MoS_2/Ag	aerosol-jet printing	120	25
63	Gr/MoS_2 QDNS/Gr	Spin coating	50	-
64	Pt/MoS_2/Ti	Spin coating	10^7	22

Reference 64 claims a high endurance 10^7 while only 22 data points are shown, which is not reliable. The correct characterization method of endurance measurement should be one data point per cycle, as explained in M. Lanza et al, Standards for the Characterization of Endurance in Resistive Switching Devices. ACS Nano 2021, 15, 11, 17214–17231.

Supplementary Table 4: LPE h-BN based memristor

Ref	**TE/RS medium/BE**	**Print method**	**Endurance**	**data points presented**
53	Ag/h-BN-PVOH/ITO	EHDA printing	1500	33
54	Ag/ZnO/BNNSs/Pt	Spin coating	-	-
This	Ag/h-BN/Pt	Inkjet printing	600,000	600,000
work	Ag/h-BN/Ag	Inkjet printing	11,000	11,000

References

[R1] C. Hao et al. Liquid-exfoliated black phosphorous nanosheet thin films for flexible resistive random access memory applications. *Adv. Funct. Mater.* 2016, **26**, 2016–2024.

[R2] S. Han et al. Black phosphorus quantum dots with tunable memory properties and multilevel resistive switching characteristics. *Adv. Sci.* 2017, **4**, 1600435.

[R3] Y. Hsieh et al. Solution-processed black phosphorus nanoflakes for integrating nonvolatile resistive random access memory and the mechanism unveiled. *Nanotechnology* 2019, **30**, 445702.

[R4] C. L. He et al. Nonvolatile resistive switching in graphene oxide thin films. *Appl. Phys. Lett.* **95**, 232101 (2009)

[R5] G. Liu et al. Bistable electrical switching and electronic memory effect in a solution-processable graphene oxide-donor polymer complex. *Appl. Phys. Lett.* 2009, **95**, 253301.

[R6] H. Y. Jeong et al. Graphene oxide thin films for flexible nonvolatile memory applications. *Nano Lett.* 2010, **10**, 11, 4381–4386

[R7] S. K. Hong et al. Flexible resistive switching memory device based on graphene oxide. *IEEE Electron Device Lett.* 2010, **31**, 1005–1007.

[R8] Y. Lai et al. Low operation voltage macromolecular composite memory assisted by graphene nanoflakes. *J. Mater. Chem. C*, 2013, **1**, 552–559.

[R9] S. K. Hong et al. Analysis on switching mechanism of graphene oxide resistive memory device. *J. Appl. Phys.* 2011, **110**, 044506.

[R10] K.S. Vasu, S. Sampath, A.K. Sood. Nonvolatile unipolar resistive switching in ultrathin films of graphene and carbon nanotubes, *Solid State Commun.* 2011, **151**, 1084-1087.

[R11] F. Zhuge et al. Mechanism of nonvolatile resistive switching in graphene oxide thin films, *Carbon* 2011, **49**, 3796–3802.

[R12] B. Hu et al. Electrically controlled electron transfer and resistance switching in reduced graphene oxide noncovalently functionalized with thionine. *J. Mater. Chem.* 2012, **22**, 16422–16430.

[R13] C. Jin et al. Nonvolatile resistive memory of ferrocene covalently bonded to reduced graphene oxide. *Chem. Commun.* 2012, **48**, 4235–4237.

[R14] G. Venugopal, S. J. Kim. Observation of Nonvolatile Resistive Memory Switching Characteristics in Ag/Graphene-Oxide/Ag Devices. *J. Nanosci. Nanotechnol.* 2012, **12**, 8522–8525.

[R15] L. Wang et al. The mechanism of the asymmetric SET and RESET speed of graphene oxide based flexible resistive switching memories. *Appl. Phys. Lett.* 2012, **100**, 063509.

[R16] S. M. Jilani, et al. Studies on resistive switching characteristics of aluminum/graphene oxide/semiconductor nonvolatile memory cells, *Carbon* 2013, **64**, 187–196,

[R17] G. Khurana, et al. Forming free resistive switching in graphene oxide thin film for thermally stable nonvolatile memory applications. *J. Appl. Phys.* 2013, **114**, 124508.

[R18] N. T. Ho et al. Impedance spectroscopy analysis of the switching mechanism of reduced graphene oxide resistive switching memory. *Solid-State Electron.* 2014, **94**, 61–65

[R19] H. Tian et al. Cost-effective, transfer-Free, flexible resistive random access memory using laser-scribed reduced graphene oxide patterning technology. *Nano Lett.* 2014, **14**, 3214–3219.

[R20] M. Yi et al. Temperature dependence of resistive switching behaviors in resistive random access memory based on graphene oxide film. *Nanotechnology* 2014, **25**, 185202.

[R21] D. H. Yoo et al. Effect of copper oxide on the resistive switching responses of graphene oxide film. *Curr. Appl. Phys.* 2014, **14**, 1301-1303.

[R22] I. Banerjee et al. Graphene oxide thin films for resistive memory switches. *IET Circuits Devices Syst.* 2015, **9**, 428–433.
[R23] H. Kim et al. Transparent multi-level resistive switching phenomena observed in ITO/RGO/ITO memory cells by the Sol-Gel Dip-Coating method. *Sci. Rep.* 2014, **4**, 4614.
[R24] S. Kim et al. Direct Observation of conducting nanofilaments in graphene-oxide-resistive switching memory. *Adv. Funct. Mater.* 2015, **25**, 6710–6715.
[R25] A. Midya et al. Flexible and transparent resistive switching devices using Au nanoparticles decorated reduced graphene oxide in polyvinyl alcohol matrix. *Curr. Appl. Phys.* 2015, **15**, 706–710.
[R26] S. Porro, C. Ricciardi. Memristive behaviour in inkjet printed graphene oxide thin layers. *RSC Adv.* 2015, **5**, 68565–68570.
[R27] H. Y. Wu et al. Characteristics of graphene-oxide-based flexible and transparent resistive switching memory. *Ceram. Int.* 2015, **41**, S823–S828.
[R28] D. Yeo et al. Nonvolatile memory devices based on Au/graphene oxide nanocomposites with bilateral multilevel characteristics. *Carbon* 2015, **88**, 26-32.
[R29] P. Hazra et al. Gate controllable resistive random access memory devices using reduced graphene oxide. *Appl. Phys. Lett.* 2016, **108**, 153503.
[R30] L. Wang et al. Controllable multiple depression in a graphene oxide artificial synapse. *Adv. Electron. Mater.* 2017, **3**, 1600244.
[R31] S. K. Kim et al. Conductive graphitic channel in graphene oxide-based memristive devices. *Adv. Funct. Mater.* 2016, **26**, 7406–7414.
[R32] P. Hazra, A. N. Resmi, K. B. Jinesh. Gate controllable resistive random access memory devices using reduced graphene oxide. *Appl. Phys. Lett.* 2016, **108**, 153503.
[R33] G. M. Khanal et al. A ZnO-rGO composite thin film discrete memristor. *IEEE International Conference on Semiconductor Electronics (ICSE)* 2016, 129–132,
[R34] S. Pradhan et al. Resistive switching behavior of reduced graphene oxide memory cells for low power nonvolatile device application. *Sci. Rep.* 2016, **6**, 26763.
[R35] V. K. Nagareddy et al. Multilevel Ultrafast Flexible Nanoscale Nonvolatile Hybrid Graphene Oxide–Titanium Oxide Memories. *ACS Nano* 2017, **11**, 3, 3010–3021.
[R36] R. Shi et al. Fully solution-processed transparent nonvolatile and volatile multifunctional memory devices from conductive polymer and graphene oxide. *Adv. Electron. Mater.* 2017, **3**, 1700135.
[R37] G. Anoop et al. Resistive switching in ZnO nanorods/graphene oxide hybrid multilayer structures. *Adv. Electron. Mater.* 2017, **3**, 1600418.
[R38] L. Wang et al. Controllable multiple depression in a graphene oxide artificial synapse. *Adv. Electron. Mater.* 2017, **3**, 1600244.
[R39] S. Kim et al. In Situ observation of resistive switching in an asymmetric graphene oxide bilayer structure. *ACS Nano* 2018, **12**, 7, 7335–7342.
[R40] Y. Park et al. Reduced Graphene Oxide-Based Artificial Synapse Yarns for Wearable Textile Device Applications. *Adv. Funct. Mater.* 2018, **28**, 1804123.
[R41] A. S. Sokolov et al. Silver-Adapted Diffusive Memristor Based on Organic Nitrogen-Doped Graphene Oxide Quantum Dots (N-GOQDs) for Artificial Biosynapse Applications. *Adv. Funct. Mater.* 2019, **29**, 1807504.
[R42] R. Vartak et al. Study of Ag/RGO/ITO sandwich structure for resistive switching behavior deposited on plastic substrate. *Appl. Nanosci*. 2018, **8**, 1343–1351.
[R43] P. J. Jesuraj et al. Improved performance of graphene oxide based resistive memory devices through hydrogen plasma, *Mater. Lett.* 2018, **232**, 62-65,
[R44] R. Singh et al. Enhanced resistive switching in graphene oxide based composite thin film for nonvolatile memory applications. *Mater. Res. Express* 2019, **6**, 105621.

[R45] T. Aziz, et al. Transparent hybrid ZnO-graphene film for high stability switching behavior of memristor device. *Mat. Sci. Semicon. Proc.* 2019, **89**, 68–76
[R46] Li, L. Tunable memristic characteristics based on Graphene Oxide charge-trap memory. *Micromachines* 2019, **10**, 151.
[R47] F. Romero et al. Laser-fabricated reduced graphene oxide memristors. *Nanomaterials* 2019, **9**, 897.
[R48] G. Khurana et al. Non-polar and complementary resistive switching characteristics in graphene oxide devices with gold nanoparticles: diverse approach for device fabrication. *Sci. Rep.* 2019, **9**, 15103.
[R49] K. Kumari et al, Structural and resistive switching behaviour in lanthanum strontium manganite - Reduced graphene oxide nanocomposite system, *J. Alloys and Compd.* 2020, **815**, 152213,
[R50] K. K. Gogoi, A. Chowdhury. Performance enhancement of solution-processed organic memories by exploiting synergistic organic–inorganic hybrid composites. *J. Phys. Chem. C* 2020, **124**, 1108–1120.
[R51] C. Tan et al. Non-volatile resistive memory devices based on solution-processed ultrathin two-dimensional nanomaterials. *Chem. Soc. Rev.* 2015, **44**, 2615.
[R52] D. Yeo et al. Nonvolatile memory devices based on Au/graphene oxide nanocomposites with bilateral multilevel characteristics. *Carbon* 2015, **88**, 26–32.
[R53] G. U. Siddiqui et al. A two-dimensional hexagonal boron nitride/polymer nanocomposite for flexible resistive switching devices. *J. Mater. Chem. C* 2017, **5**, 862–871.
[R54] G. Wang et al. Memristors based on the hybrid structure of oxide and boron nitride nanosheets combining memristive and neuromorphic functionalities. *Phys. Status Solidi RRL* 2020, 14, 1900539.
[R55] J. Liu et al. Preparation of MoS2-Polyvinylpyrrolidone nanocomposites for flexible nonvolatile rewritable memory devices with reduced graphene oxide electrodes. *Small* 2012, **8**, 3517–3522.
[R56] X. Xu et al. Resistive switching memories in MoS2 nanosphere assemblies. *Appl. Phys. Lett.* 2014, **104**, 033504.
[R57] A. Bessonov et al. Layered memristive and memcapacitive switches for printable electronics. *Nat. Mater.* 2015, **14**, 199–204.
[R58] D. Son et al. Colloidal synthesis of uniform-sized molybdenum disulfide nanosheets for wafer-Scale flexible nonvolatile memory. *Adv. Mater.* 2016, **28**, 9326–9332.
[R59] D. Wang et al. Quantum conductance in MoS2 quantum dots-based nonvolatile resistive memory device. *Appl. Phys. Lett.* 2017, **10**, 093501.
[R60] Y. Zhai et al. Infrared-sensitive memory based on direct-grown MoS2 upconversion nanoparticle heterostructure. *Adv. Mater.* 2018, **30**, 1803563.
[R61] B. Yalagala et al. Ultra-low cost, large area graphene/MoS2-Based piezotronic memristor on paper: A systematic study for both direct current and alternating current inputs. *ACS Appl. Electron. Mater.* 2019, **1**, 883–891.
[R62] X. Feng et al. A fully printed flexible MoS2 memristive artificial synapse with femtojoule switching energy. *Adv. Electron. Mater.* 2019, **5**, 1900740.
[R63] X. Fu et al. Molybdenum disulfide nanosheet/quantum dot dynamic memristive structure driven by photoinduced phase transition. *Small* 2019, **15**, 1903809.
[R64] B. Tang et al. Wafer-scale solution-processed 2D material analog resistive memory array for memory-based computing. *Nat. Commun.* 2022, 13, 3037.